

2D WS₂ Embedded PVDF Nanocomposites for Photosensitive Piezoelectric Nanogenerators with a Colossal Energy Conversion Efficiency ~ 25.6%

Didhiti Bhattacharya¹, Sayan Bayan^{1,#}, Rajib Kumar Mitra¹ and Samit K. Ray^{*1,2}

¹ S. N. Bose National Centre for Basic Sciences, Kolkata, 700106, West Bengal, India

² Indian Institute of Technology Kharagpur, 721302, West Bengal, India

[#]Present address: Department of Physics, Rajiv Gandhi University, Arunachal Pradesh 791112, India

* e-mail : physkr@phy.iitkgp.ac.in

Supporting information:

Synthesis of WS₂ nanosheets:

WS₂ nanosheets are chemically exfoliated by using Li-intercalation technique. Bulk WS₂ powder 2.5 gm with anhydrous LiBr at 1:1 molar ratio are dispersed in 20ml hexane solution. This solution is sonicated for 4 hrs by using bath sonicator. After sonication the resulting black dispersion is centrifuged at 4000 rpm for 10 mins to remove hexane and untreated Li ions. The wet sediments are washed by dispersing in DMF by shaking followed by centrifugation. By repeating this procedure twice the wet sediment of WS₂ is completely transferred in DMF solvent. The final exfoliation is done in DMF by bath sonication for 1hr. Then the resulting solution is centrifuged at 5000 rpm for 10min and greenish colour exfoliated WS₂ nanosheets are obtained.

Characterizations of WS₂ nanosheet:

Fig.S1 (a) shows the TEM image of the exfoliated WS₂ nanosheets. HRTEM in Fig.S1(b) shows the lattice fringe pattern with an inter-planar spacing of 0.27 nm for the (100) plane and 0.62 nm for (002) plane of the 2H-WS₂ nanosheets. The HRTEM Fig.S1(c) and Selected area electron diffraction pattern of WS₂ flakes in Fig.S1(d) indicates the hexagonal atomic arrangement of 2H-WS₂ nanosheets. The AFM image in Fig.S1(e) indicates that the exfoliated WS₂ nanosheets are few layered in thickness. In the absorbance spectrum characteristic peaks are observed at 628 nm, 523 nm, 452 nm and 409 nm marked as A, B, C and D, respectively³ in Fig.S2(a). In Raman spectrum two characteristics modes of vibration A_{1g} and E¹_{2g} of WS₂ assigned to the out-of-plane

and in-plane vibrations of the W and S atoms, respectively, are shown in Fig.S2(b). The characteristic peaks for A_{1g} and E_{12g} vibrations are observed at 417.4 and 352.8 cm^{-1} respectively, for the exfoliated WS_2 . Both the absorbance and raman spectrum agrees with formation of few layered exfoliated WS_2 nanosheets. The XRD diffraction peak at 14.4° indicates the formation of (002) plane of WS_2 nanosheet which indicates the good crystallinity of exfoliated WS_2 nanosheets.

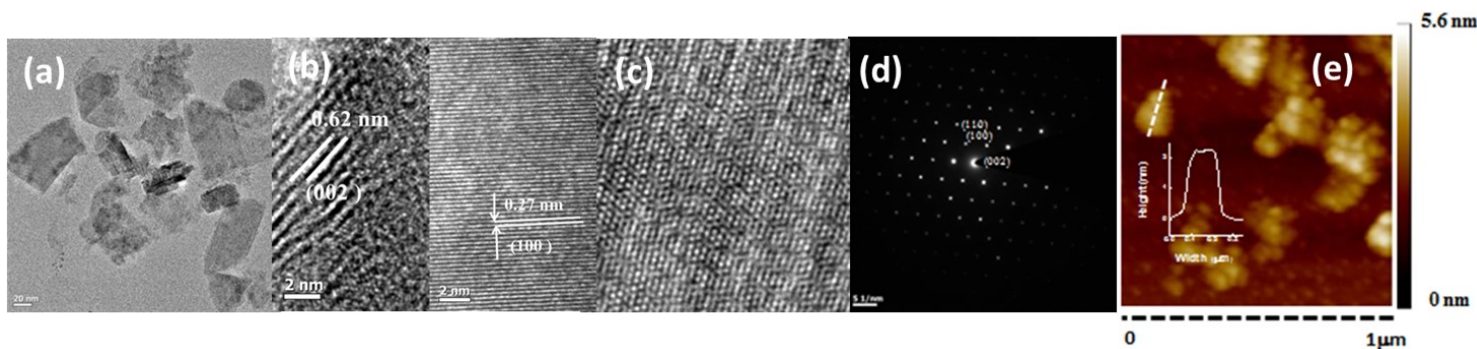


Fig.S1 (a) TEM image of exfoliated WS_2 nanosheets, HRTEM image of WS_2 nanosheet indicating (b) inter planer (100) spacing of 0.27 nm, (002) of 0.62 nm and, (c) hexagonal atomic orientation, (d) Selected area diffraction pattern showing the crystallinity of WS_2 nanosheets, (e) AFM image of WS_2 nanosheets and the high profile of a single sheet.

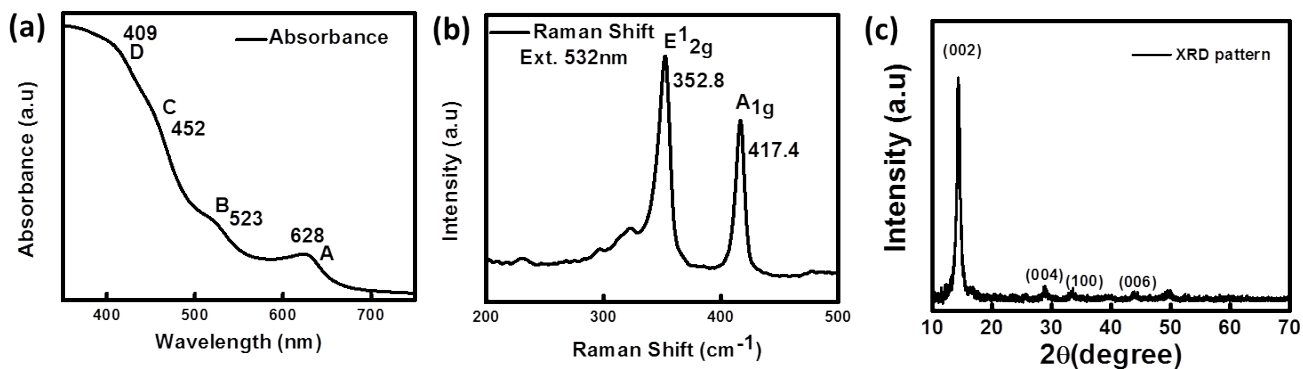


Fig.S2 (a) Absorption spectrum, (b) Raman spectrum, (c) XRD pattern of synthesized WS_2 nanosheets.

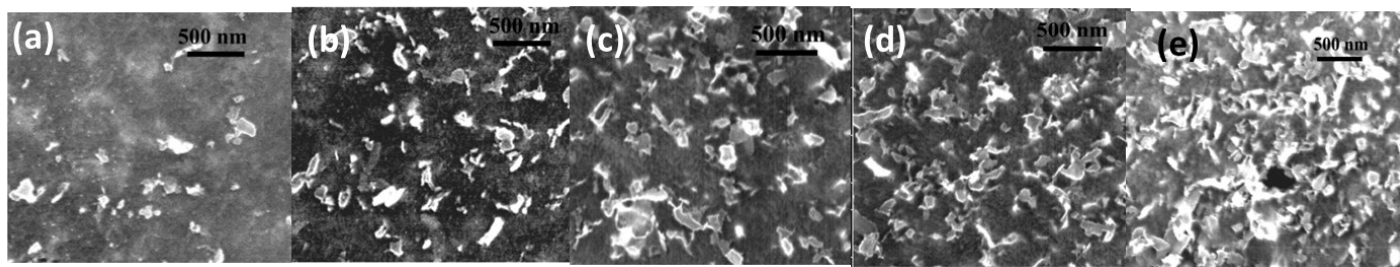


Fig.S3 SEM images of PVDF-WS₂ nanocomposite for filler loading (a) 0.03%,(b) 0.07%,(c) 0.12%, (d) 0.18% and (e) 0.26%

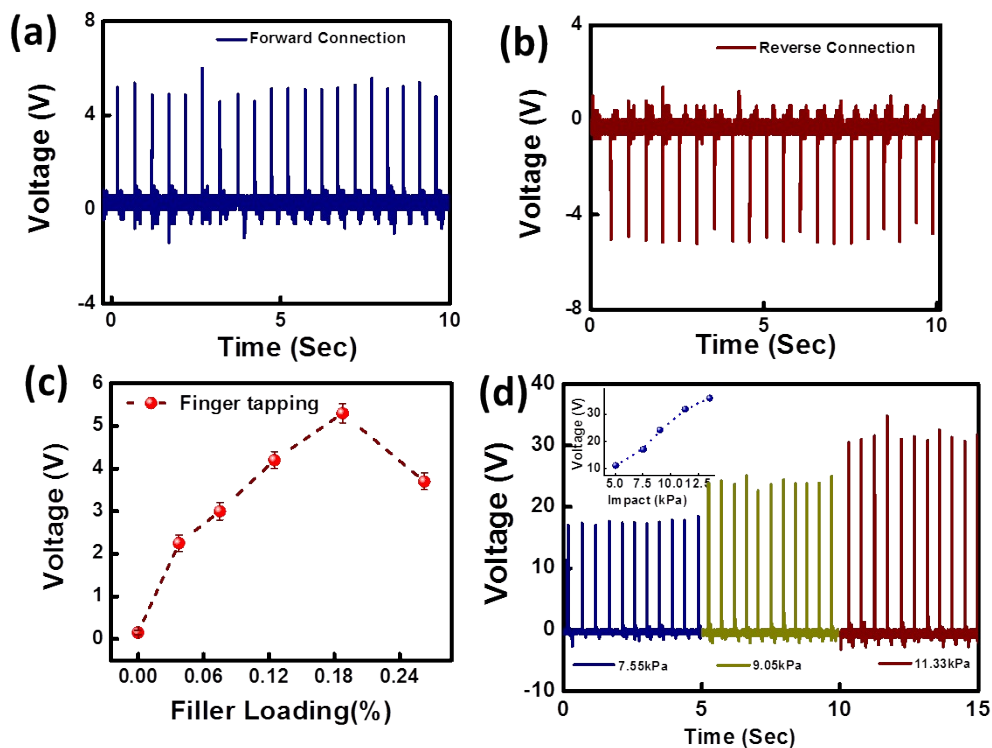


Fig.S4 Open-circuit output voltage from PVDF-WS₂ PENG in (a) forward, (b) reverse connection, (c) variation of open circuit output voltage due to variation of filler loading, (d) variation of open circuit output voltage with variation of mechanical impact.

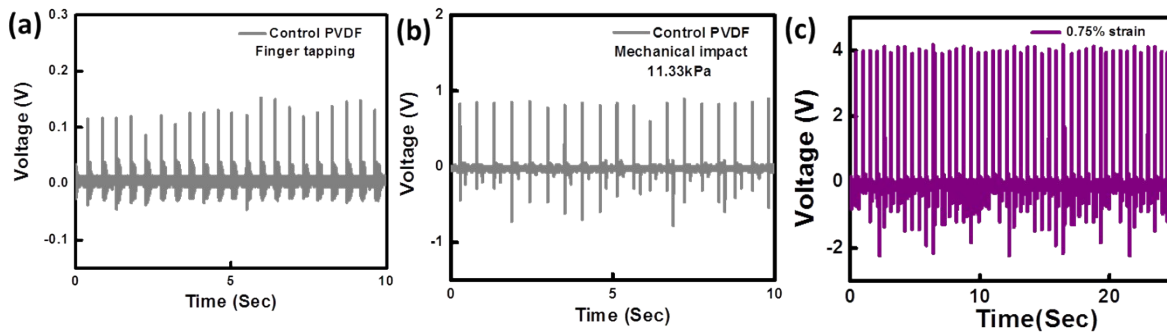


Fig.S5 Open-circuit output voltage from control PVDF device from (a) finger tapping, (b) mechanical impact (11.33 kPa), (c) open circuit output voltage from PVDF-WS₂ PENG device under repeated bending-releasing cycle.

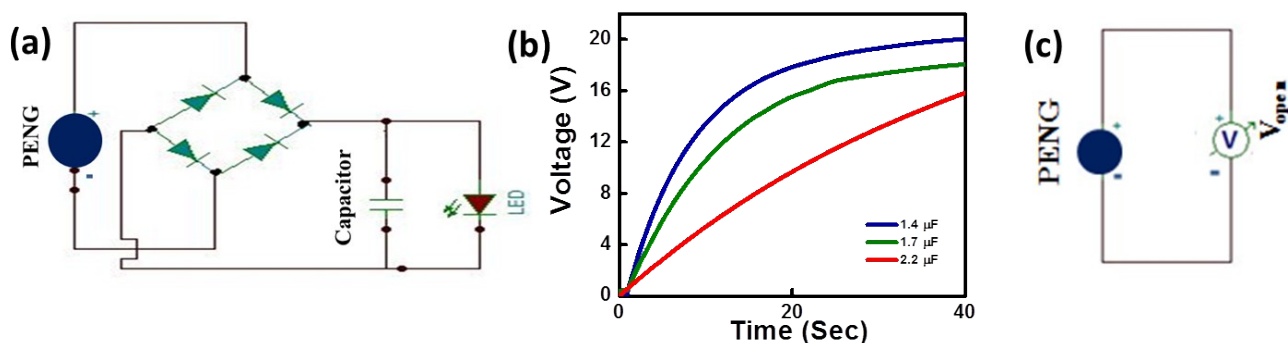


Fig.S6 (a) Schematic circuit for charging of capacitor and LED glowing, (b) V-t characteristic for charging of capacitors, (c) Schematic circuit for measuring open circuit voltage from the PENG.

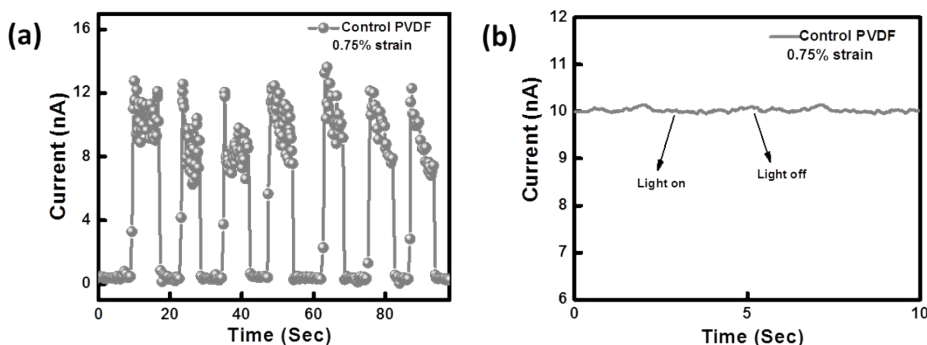


Fig.S7 I-t characteristic from control PVDF device (a) under application of repeated bending and releasing at 0.75% strain, (b) change of current for light on-off at 0.75% strain.

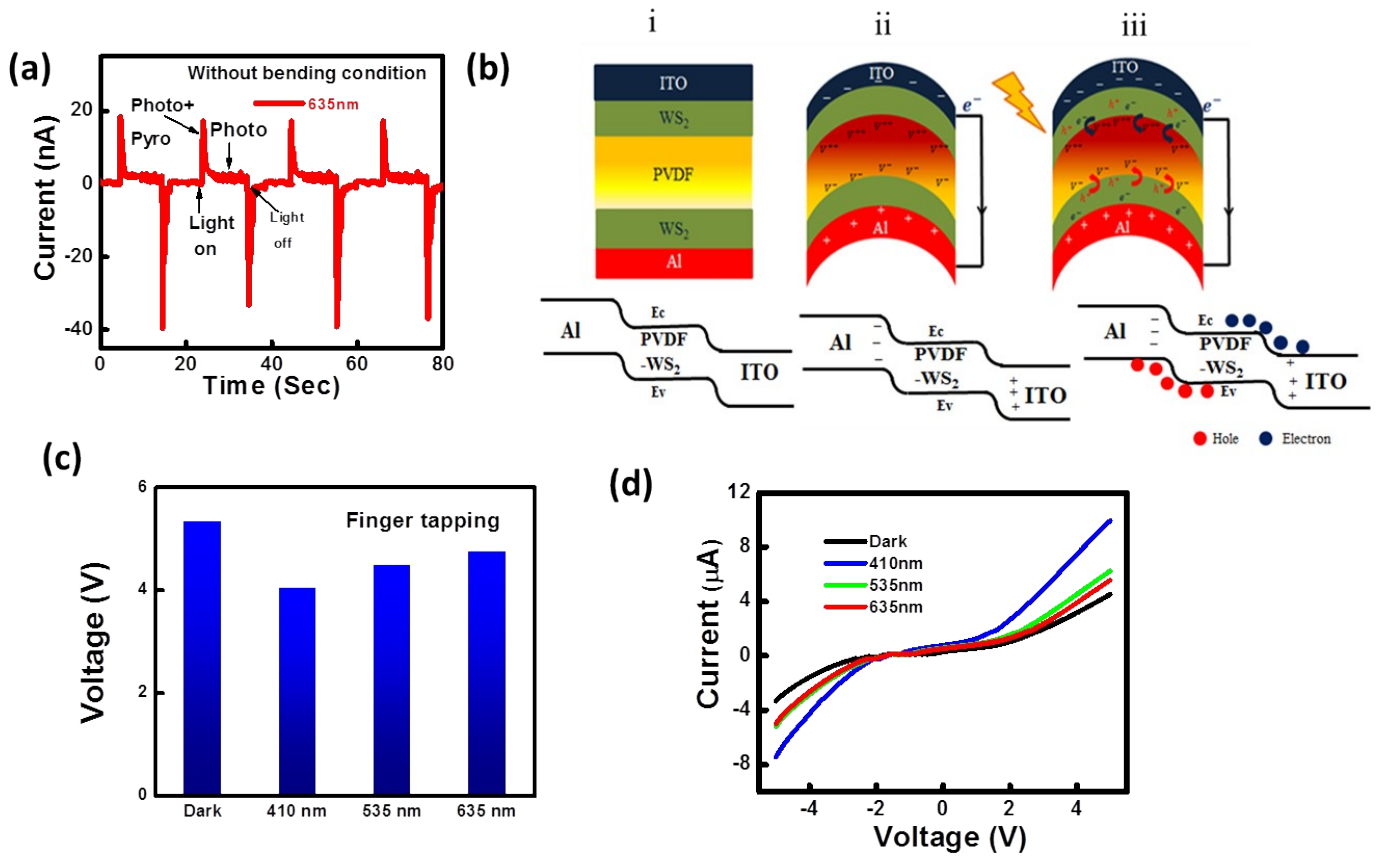


Fig.S8(a) I-t characteristic at zero bias without bending under 635 nm illumination, (b) schematic working mechanism of piezo-photo coupled system.(c) variation of open circuit voltage at dark and illuminated condition, (d) I-V characteristic of the PENG under dark and illuminated conditions.

The photosensing behavior of PVDF-WS₂nanocomposites has been investigated without the application of any external bias and external bending strain, the output signal presented in Fig. S8(a) observed under periodic illumination (~635 nm, 0.4 mW/ cm²).To establish the mechanism of the piezo-phototronic effect in PENG, the energy band diagrams of the device under strain free and strained condition in dark and illuminated conditions have been analyzed. It can be observed that in the absence of any external stress, molecular dipoles within the nanocomposite are randomly oriented, and therefore it does not possess any net field (Fig.S8(b)i). Under application of an external stress, the piezoelectric dipolar charges are aligned along the stress

induced direction leading to the generation of piezopotential across the electrodes (Fig.S8(b)ii), and this resultant piezoelectric potential drives the electrons in the external circuit and develops a voltage pulse as well as also generates a piezo-current. When the illumination energy is comparable to the band-gap of WS₂ nanosheet, light induced e-h pairs are generated inside the nanocomposite and they are separated by the built-in piezoelectric field. As the result the light induced photocarriers reduce the strain induced piezopotential. Thus the screening of piezo-charges by the photogenerated e-h pairs takes place and the redistributed piezoelectric charges appear across the opposite electrodes (Fig.S8(b)iii). The open circuit output voltages are found to be reduced in illuminated condition with respect to that in the dark under an identical external force (finger tapping) at periodic intervals (2Hz). The reduction of open circuit output voltage in illuminated condition under different wavelength is presented in Fig.S8(c). From Fig.S8(d) it is observed that there is finite enhancement of current under illuminated conditions than the dark, which indicates the enhanced photo-carrier density and reduced internal resistance of the PENG under light illumination than the dark condition. It can be noted that the power density attains maximum value under ~ 2MΩ load resistance at dark condition and 0.76MΩ, 1.08MΩ, 1.3MΩ under illumination of 410nm, 535nm and 635 nm respectively.

Strain calculation (Bending)

In this experiment, the mechanical strain (ϵ) in bended condition has been generated by a home-made bending set up as shown below. The strain on the film can be calculated upon considering the film thickness and the effective bending radius (schematically represented in the below figure) following the relation [Ref 37]

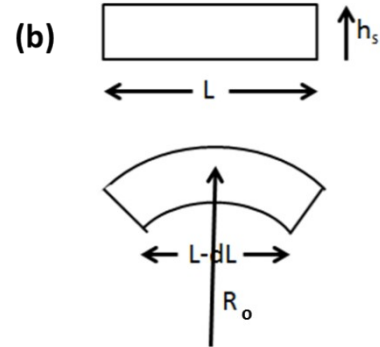
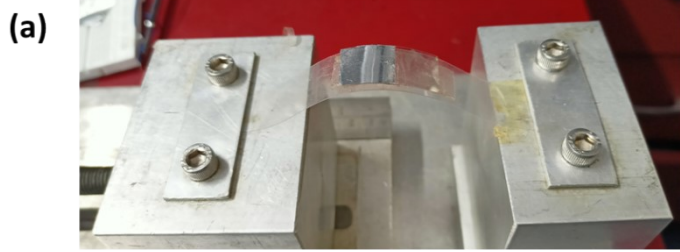
$$\epsilon = \frac{h_s}{2R_o} \text{ where } h_s \text{ is the thickness of the device } \sim 150 \mu\text{m} \text{ and } R_o \text{ is the bending radius}$$

$$R_o = \frac{L}{2\pi \sqrt{\frac{dL}{L} - \frac{\pi h_s^2}{12L^2}}}$$

Where L is the undeformed original length, dL is the change of length upon bending.

For example $L=3.0$ cm, $dL=0.5$ cm $R_o=1.17$ cm

$$\varepsilon=6.39 \times 10^{-3} \sim 0.64\%$$



(a) Image of bending set up with device, (b) schematic representation of radius of curvature

Calculation of Young's modulus:

We have used mixing rule to estimate the Young's modulus of the nanocomposite [Ref 53]

$$E_c = fE_f + (1 - f)E_m$$

Where f is filler fraction $\sim 0.18\%$, E_f is the Young's modulus of filler ~ 272 GPa, E_m is the Young's modulus of matrix ~ 2.17 GPa, $E_c \sim 2.66$ GPa